Accurate Evaluation of a Millimeter Wave Compact Range Using Planar Near-Field Scanning

ANDREW G. REPJAR, MEMBER, IEEE, AND DOUGLAS P. KREMER

Abstract—**Significant progress has been made in recent years on planar near-field measurements for antenna calibrations. Such measurements are also useful in the alignment and evaluation of compact ranges because they provide more information than a limited number of analogue plots in one dimension. Contour plots of amplitude and phase data obtained from more complete two-dimensional measurements precisely and accurately locate sources of problems in the range reflector, with phase contour plots being more useful as diagnostic tools.**

I. INTRODUCTION

CONSIDERABLE PROGRESS has been made in the last decade on the development of compact ranges for antenna and radar cross-section measurements but primarily at frequencies below 30 GHz [1]. Range development at frequencies approaching 100 GHz has largely been hindered by the cost and availability of a suitable precision parabolic reflector, one of the most critical elements in compact range design. Compact ranges offer the advantages of a closed environment and the direct measurement of far-field antenna and radar cross section patterns. For radar cross-section measurements of scaled models, extending the frequency range to 100 GHz will enable use of scaling factors approximately ten times larger than currently employed. Hence, radar cross sections of much larger objects can be determined. For antenna measurements at frequencies approaching 100 GHz, the closed-environment feature of a compact range could strongly favor its use over a far-field range, while the direct-measurement feature could be an advantage for the compact range over the near-field scanning method which could require a large number of measurement points and long fast Fourier transform (FFT) processing times [2].

The goal for the effort discussed in this paper was to develop a compact range that would provide an approximate plane wave illumination over a measurement zone 120 cm^2 with less than 0.5 dB amplitude variation and less than 10° phase variation at any frequency in the 12 to 100 GHz range. The system utilizes a segment of a parabolic reflector approximately 450 cm by 450 cm to provide the plane wave illumination of a target. The results of planar near-field measurements [3] on this compact range demonstrate that the goal can be achieved for two preselected test frequencies, namely 18.0 and 54.75 GHz.

In this paper, the specifications for the reflector size, shape, and surface tolerances are discussed along with the factors considered in choosing the particular reflector that was selected for the compact range. Next, the specifications of the feeds and a discussion of the feeds subsequently obtained are presented. The measurement approach is then described and is followed by the alignment procedure for the compact range. The next section describes and interprets the measurements obtained with both narrow-beam and wide-beam probes and also includes results for cross-component measurements. Conclusions are then presented.

Manuscript received October 27, 1980; revised June 15, 1981.

The authors are with the Electromagnetic Fields Division, Center for Electronics and Electrical Engineering, Bureau of Standards, Boulder, CO 80303.

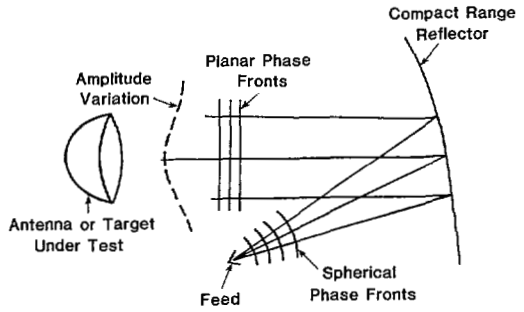

Fig. 1. Compact range schematic. Following D. Hess, lecture notes on the Compact Range, Microwave Antenna Measurements Short Course, California State University, Northridge, July 1977.

II. REFLECTOR

A precision parabolic reflector is one of the most critical elements in compact range design. Johnson *et al.* [4] adequately pointed out that the problem areas to be considered for designing a compact range reflector include depolarization, space attenuation from the feed, diffraction from reflector edges, and surface tolerances, which are most important. The surface tolerances are particularly critical for a compact range which is designed to operate up to 100 GHz at which frequency the wavelength is 3000 μm. At this frequency, in order to achieve accuracies in phase in the order of 10° in the planar wavefronts (see Fig. 1), surface accuracies on the order of 83 μm (1/36 of a wavelength) are required. In addition, as pointed out in [4], to obtain small variations in amplitude on the order of 0.5 dB, i.e., uniform amplitude distribution, surface accuracies of about 0.007 of a wavelength, or 20 μm at 100 GHz, are required—a demanding specification.

Chu and Turrin [5] have calculated the cross polarization of a linearly polarized excitation for offset reflectors and show how the cross component decreases with increasing focal length. The space attenuation effect also decreases with increasing focal length [4], so it is advantageous for the compact range reflector to have a long focal length. For a parabolic reflector approximately 450 cm square, the minimum focal length of the reflector should be about 450 cm which would give a maximum cross polarization for linear polarized excitation of about −30 dB, see [5, Fig. 3].

Hess *et al.* [1] have demonstrated the effectiveness of serrated edges (as opposed to straight edges) on the reflector in reducing the diffracted power in the measurement zone. This also was considered in choosing the reflector surface.

Upon consideration of the surface tolerance and focal length specifications, the reflector used for this compact range

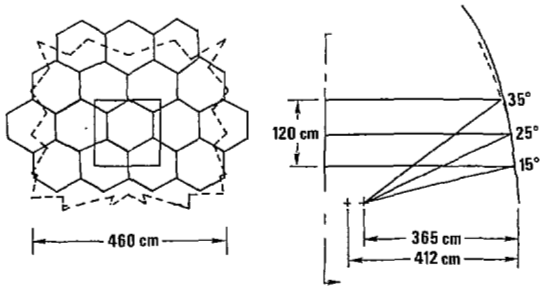

—— Reflector 1, 450 cm × 360 cm (approx.) dish, irregular edges, 30 μm surface tolerance, hexagonal panels, focal length = 412.32 cm.
····· Reflector 2, 450 cm × 360 cm (approx.) dish, serrated edges, focal length ≃ 365 cm.

Fig. 2. Overlay of schematics for compact range reflector 1 and reflector 2 (see text).

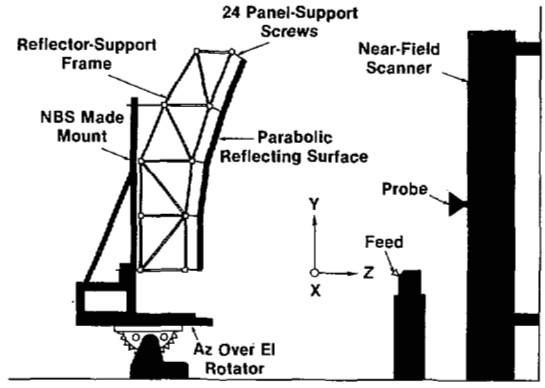

Fig. 3. Measurement facility schematic and coordinate system, compact range, NBS, Boulder, CO.

is a portion (16 panels) of a precision 10-m diameter reflecting surface originally part of a prototype telescope for millimeter and submillimeter radio astronomy [6]. Each hexagonal panel has a surface accuracy of about 50 μm root mean square (rms), and the focal length of the reflector is 412.32 cm. The reflector support frame can be disassembled and reassembled and the panels reattached, and the original parabolic surface accuracy can be obtained by adjusting 24 panel-support screws which provide an adjustment of 317.5 μm per revolution. A schematic of the reflector is shown in Fig. 2 along with an overlay (approximate) of the reflector used by Hess for comparison.

III. FEED ANTENNAS

The compact range is to provide an approximately plane wave illumination over a measurement zone 120 cm square with less than 0.5 dB variation. From Fig. 2 it can be seen that the 0.5 dB beamwidth of the feed should be a minimum of 20°. Also, as discussed in [4], direct radiation from the feed to the measurement zone can be a serious problem. Hence the feed should be designed with low radiation in the direction of the measurement zone. It should be noted that the judicious placement of high-quality absorbing material can reduce this radiation.

To satisfy the above criteria, scalar feeds were chosen to illuminate the reflecting surface. At midfrequency, their *E*-plane and *H*-plane half-power beamwidths are approximately 59° and 64°, respectively, and their 0.5 dB beamwidth is in the order of 25°. At 90° off-axis, the relative power is down approximately 27 dB. The planar near-field measurements on the compact range were conducted at 18.0 and 54.75 GHz, so *Ku*- and *V*-band feeds were obtained.

IV. MEASUREMENT APPROACH

The parabolic reflecting surface, approximately 396 cm high and 475 cm wide was mounted on the azimuth-over-elevation rotator, as shown in Fig. 3, at the National Bureau of Standards (NBS) near-field facility in Boulder using the NBS-made mount. In this configuration the rotator was used to align the reflector with its axis normal to the plane of the scanner, and then the scanner was used to measure the field uniformity in a plane. The dimensions of the measurement plane of the scanner were set at 373 cm in the x-direction and 378 cm in the y-direction. The z-variation of the scanner area was previously measured to be ±127 μm. The 120 cm square measurement zone of the compact range under test was centered at $x = 185$ cm and $y = 165$ cm. A feed support allowing translation in x, y, z and rotation in elevation and azimuth was constructed. The probes used in the planar scanner included a *Ku*-band horn (12.4–18.0 GHz), a *V*-band horn (50.0–75.0 GHz), and a *Ku*-band open-ended waveguide. Their nominal gains are 24.7 dB, 25.5 dB and 6.0 dB, respectively.

Alignment of the compact range requires measuring the electromagnetic field, both amplitude and phase, in a zone approximately 150 cm behind the feed, as shown in Fig. 3. This distance was chosen after it was determined that direct radiation from the feed to a measurement zone approximately 90 cm behind the feed caused a peak-to-peak ripple in the measured amplitude of approximately 1 dB, which was unacceptable. With the measurement plane 150 cm behind the feed, the ripple amplitude was significantly reduced since the strength of the interfering signal from the feed was decreased. (The latter is due to the fact that the measurement area of the planar scanner is now completely in the reverse hemisphere of the feed where feed signal strength is least.)

A useful model which identifies the location and strength of such an interfering signal is that of an extraneous plane wave of amplitude E_R, interfering with a desired plane wave of amplitude E_D, at an angle θ from the normal (see Fig. 4). The spatial period P of the ripple is

$$P = \frac{\lambda}{\sin\theta}, \tag{1}$$

where λ is the wavelength. Hence, the angle of arrival of the intefering signal E_R is

$$\theta = \sin^{-1}\left(\frac{\lambda}{P}\right), \tag{2}$$

which may be used to locate the interfering source. The relative strength of this interfering signal is

$$\frac{E_R}{E_D}\ (\text{dB}) = 20 \log \left[\frac{-1 + \text{antilog}\left(\frac{\sigma}{20}\right)}{1 + \text{antilog}\left(\frac{\sigma}{20}\right)}\right], \tag{3}$$

where σ is the peak-to-peak ripple amplitude, i.e., the difference in dB between the maxima and minima of the meas-

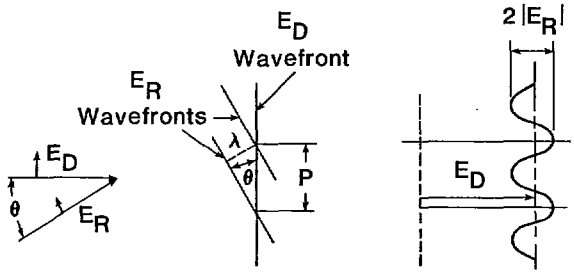

Fig. 4. Relation of field components for interaction between a single extraneous plane wave and a desired plane wave. Following Hollis *et al.*, Microwave Antenna Measurements, pp. 14–46, Scientific Atlanta, Inc., July 1970.

ured pattern. The more complete discussion of this model is available in [7 pp. 14.42–14.48].

V. ALIGNMENT PROCEDURE

Alignment of the compact range requires measuring the electromagnetic field, both amplitude and phase, in the zone approximately 150 cm behind the feed (see Fig. 3). The horn probes were chosen for the alignment and reflector evaluation because, due to their narrower beamwidths (when compared to the beamwidths of open-ended waveguide probes) they discriminate against variations caused by edge diffraction and feed spillover, and focus on the data showing reflector surface errors.

Since a planar wavefront is desired in the test zone, it is advantageous for the measurement plane of the planar near-field scanner to coincide with a measurement plane of the test zone. First, the nominal axis of the reflector is set parallel to the normal of the scanner plane, and the feed is positioned at the nominal focal point of the reflector. Then the feed is translated in x increments of approximately 1/36 of a wavelength, i.e., 0.5 mm at 18 GHz and rotated in azimuth. At the same time, the reflector is rotated in azimuth in increments of 0.01° until maximum symmetry is achieved in x for both amplitude and phase plots in the *entire* measurement plane of the near-field scanner. (At this point, it should be noted that initially, symmetry was achieved for a number of x scans over the upper and lower portions of the near-field scanner area. This indicated that *no* adjustments would have to be made in the panel-support screws affecting those regions. However, an adjustment of a panel-support screw which affects an off-center part of the middle portion of the measurement area had to be made to obtain total symmetry in x over the *entire* measurement plane and is discussed in the next section. This adjustment did not affect the alignment of the reflector in azimuth since, for this purpose, only the upper and lower measurement areas were utilized to obtain symmetry in x. In addition, this adjustment did not affect the alignment of the reflector in elevation since *only* y scans in the *center* of the measurement zone were utilized for that purpose.

In increments of approximately 0.5 mm, the feed is then translated in the z direction until the phase measurements are nearly constant in x. These results, namely before and after the translation of the feed in the z direction, are shown for $y = 335$ cm in Fig. 5 where the effect of the amplitude taper of the feed on the shape of the amplitude curve is also evident. The reflector is then rotated in elevation in increments of 0.01° and the feed is adjusted in y in small increments and in elevation angle until the phase is nearly constant in y. The

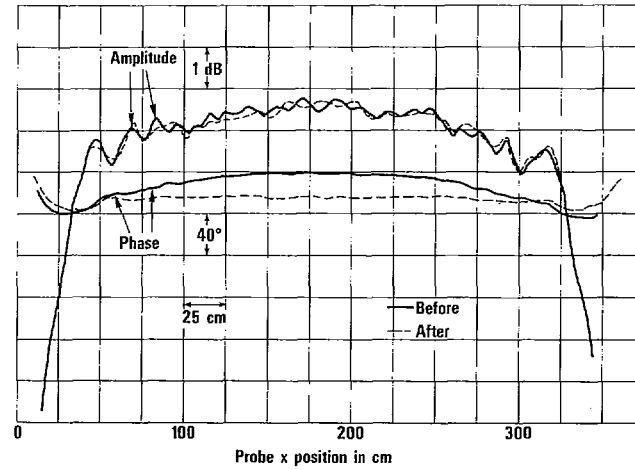

Fig. 5. Compact range main component, amplitude and phase, before and after feed translation in $-z$, x scan, $y = 335$ cm (upper portion), $f = 18.0$ GHz.

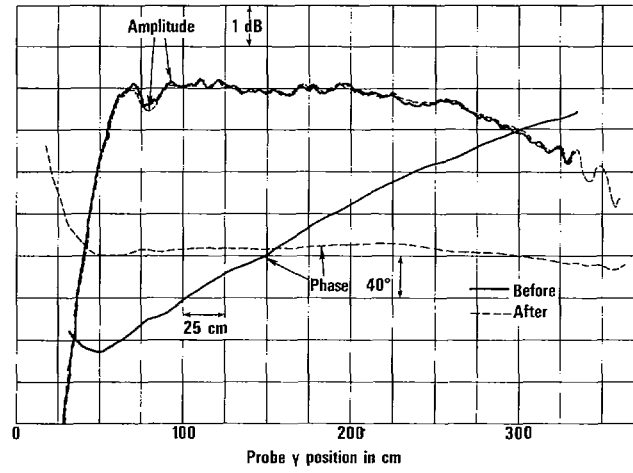

Fig. 6. Compact range main component, amplitude and phase, before and after reflector rotated in elevation, y scan, $x = 185$ cm, $f = 18.0$ GHz horn probe.

results, before and after the reflector was rotated in elevation, are presented in Fig. 6 for $x = 185$ cm. At this point, the azimuth and elevation readouts were set to zero. This alignment procedure can then be repeated so that final adjustments can be made to satisfy all the above conditions optimally and simultaneously.

VI. RESULTS

A. Using Horn Probe at 18 GHz

When the above alignment procedure was completed, both symmetry in x of the electromagnetic field amplitude, and constant phase for a number of x scans were achieved over the upper and lower portions (see Fig. 5) of the measurement area simultaneously. However, amplitude symmetry and constant phase over the middle portion were not present. Under these conditions, contour plots of amplitude and phase were obtained from complete two-dimensional data spaced 2.54 cm in both x and y, and are presented in Figs. 7 and 8, respectively. Note the unexpected concentric phase contours at the left center position. Furthermore, from the amplitude contour plot, it is evident that the symmetry in x does not exist in this left center region. The overlaying of the reflector diagram onto

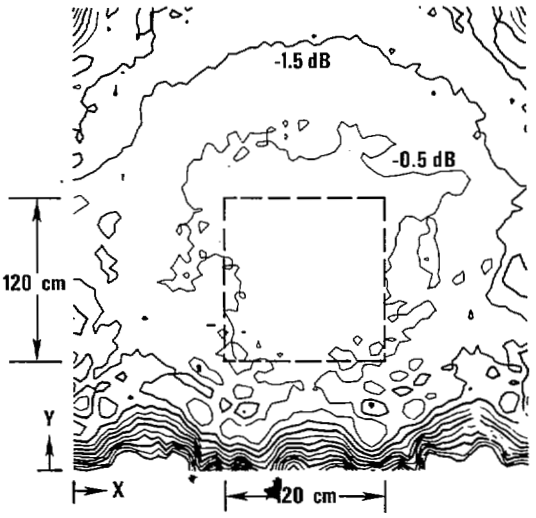

Fig. 7. Compact range main component, 1 dB amplitude contours, no panel-support screws adjusted, f = 18 GHz, horn probe.

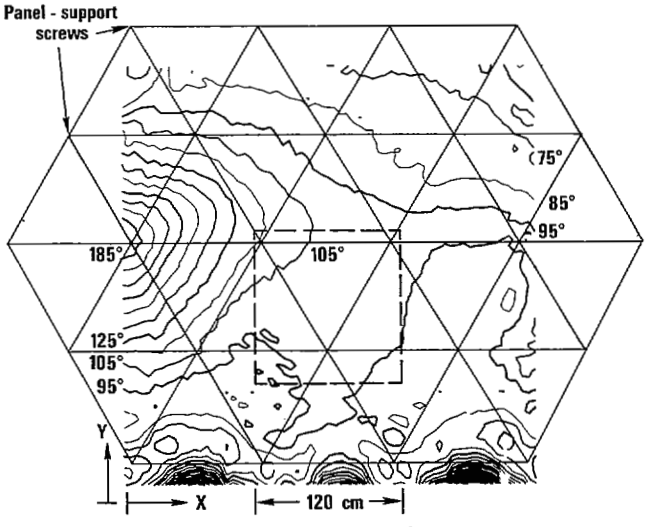

Fig. 8. Compact range main component, 10° phase contours, no panel-support screws adjusted, f = 18 GHz, reflector support overlay, horn probe.

the phase plot (Fig. 8) makes it apparent that the errors are in the vicinity of a specific support screw and are a result of the reassembly of the reflector. However, since this support screw is adjustable (317.5 μm per turn or, equivalently, 6.86°/turn at 18 GHZ), as are all 24 support screws, an adjustment was continuously made until the phase along the x scan which overlays this support screw was constant. Complete two-dimensional scans were then taken, and the resulting amplitude and phase contour plots are shown in Figs. 9 and 10. (At this point it should be noted that the alignment of this reflector and subsequent panel screw adjustment using only a limited number of analogue plots at various y positions in the middle region would have been difficult, if not impossible!) It is evident from these figures that the amplitude variations are very close to the 0.5 dB specification and that the phase is within the 10° specification over the 120 cm test zone. Also, the expected symmetries in x are quite apparent. By making more adjustments in the panel-support screws, one could have at this time improved the contour plots even further. However, it was anticipated that adjustments would be made at 54.75 GHz where the effects would more readily be seen.

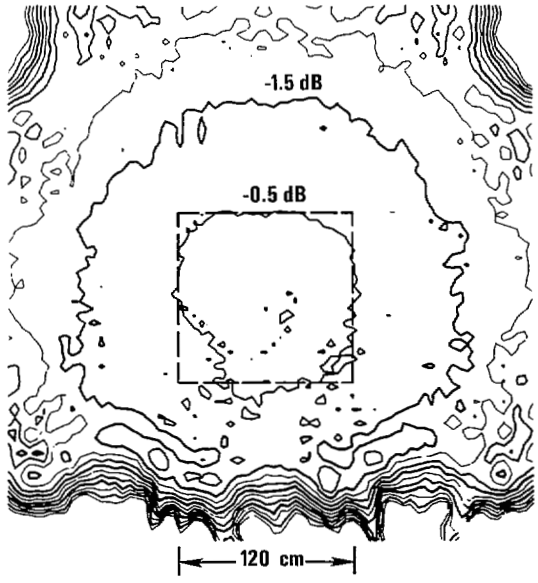

Fig. 9. Compact range main component, 1 dB amplitude contours, one panel-support screw adjusted, f = 18 GHz, horn probe.

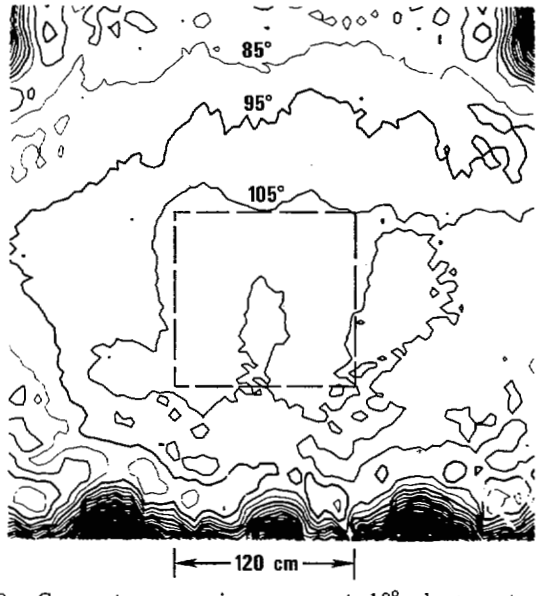

Fig. 10. Compact range main component, 10° phase contours, one panel-support screw adjusted, f = 18 GHz, horn probe.

B. Using the Horn Probe at 54.75 GHz

At 54.75 GHz, the V-band feed was installed with the center of its aperture coincident with the final location of the center of the aperture of the Ku-band feed. Complete two-dimensional data were taken and contour plots of amplitude and phase were generated and are shown in Figs. 11 and 12, respectively. In the 120 cm square test zone, although the amplitude variation is within the 0.5 dB specification, the phase varies by as much as 20°. Again though, after the reflector diagram was overlaid on the phase contour plot (Fig. 12), it became apparent that a second panel-support screw, namely the one encircled by contour lines, could be favorably adjusted. This adjustment was continuously made until the phase along the x scan which overlays that support screw was nearly constant. Complete two-dimensional data were retaken, and the new amplitude and phase contours generated are given in Figs. 13 and 14, respectively. It is evident that the phase is

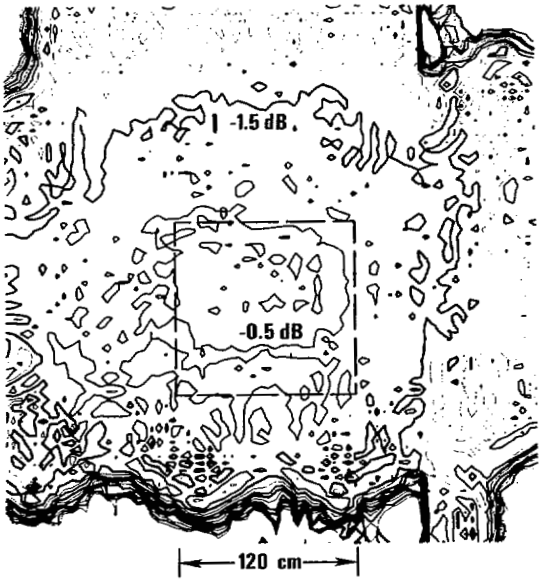

Fig. 11. Compact range main component, 1 dB amplitude contours, one panel-support screw adjusted, f = 54.75 GHz, horn probe.

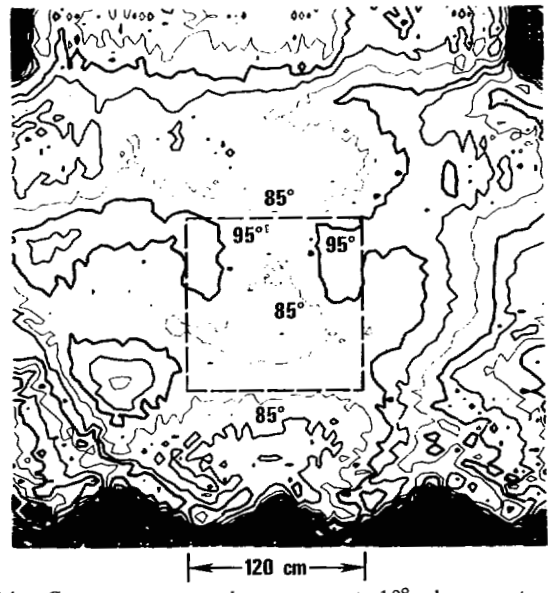

Fig. 14. Compact range main component, 10° phase contours, two panel-support screws adjusted, compact range, f = 54.75 GHz, horn probe.

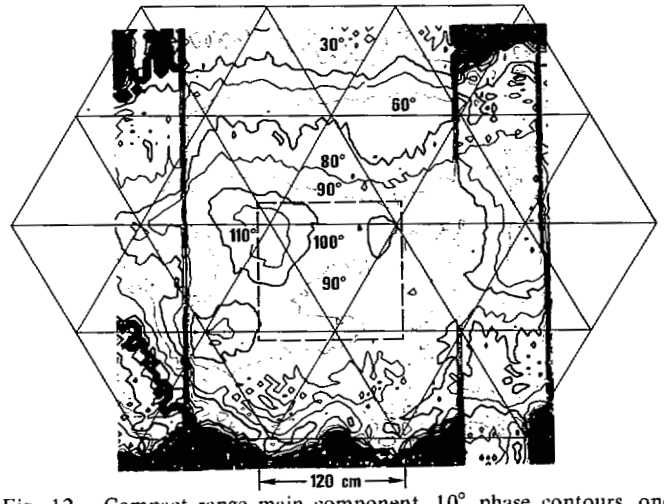

Fig. 12. Compact range main component, 10° phase contours, one panel-support screw adjusted, f = 54.75 GHz, horn probe.

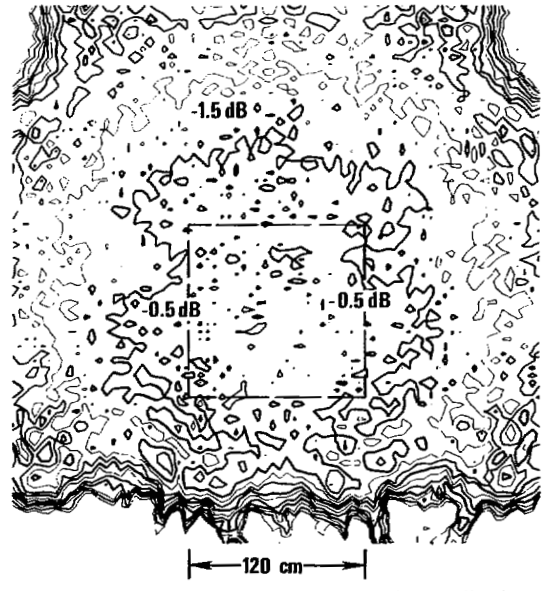

Fig. 15. Compact range main component, 1 dB amplitude contours, one panel-support screw adjusted, f = 18 GHz, waveguide probe.

Fig. 13. Compact range main component, 1 dB amplitude contours, two panel-support screws adjusted, f = 54.75 GHz, horn probe.

indeed improved over that shown in Fig. 12 since the phase variation now is in the order of 10°. Furthermore, upon comparing the final phase contours in the test zone, obtained at 18 GHz (Fig. 10), with the phase contours in Fig. 12, obtained at 54.75 GHz, one can conclude that this second panel-support screw adjustment would reduce the phase variation at 18 GHz in a manner similar to that observed in figure 14 at 54.75 GHz. Hence, the phase variation at 18 GHz might be in the order of 5°.

C. Using Waveguide Probe at 18.0 GHz

After measurements were taken at 18 GHz with the horn probe, the broader beam open-ended waveguide was utilized. Complete two-dimensional scans were obtained, and the contour plots of the measured amplitude and phase are presented in Figs. 15 and 16. It is evident that the amplitude and phase have higher frequency variations than those obtained with the

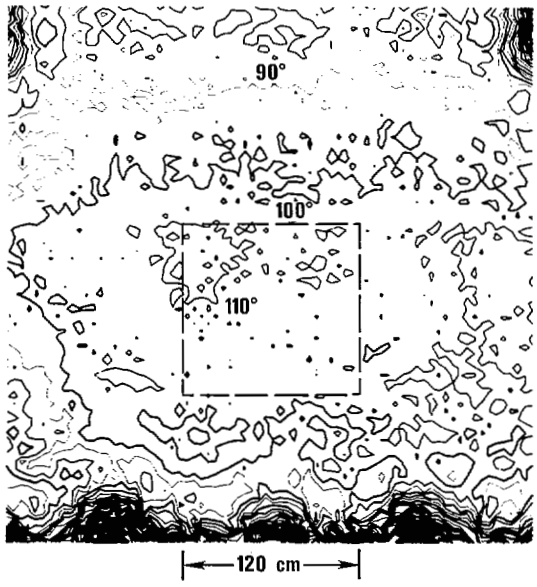

Fig. 16. Compact range main component, 10° phase contours, one panel-support screw adjusted, f = 18 GHz, waveguide probe.

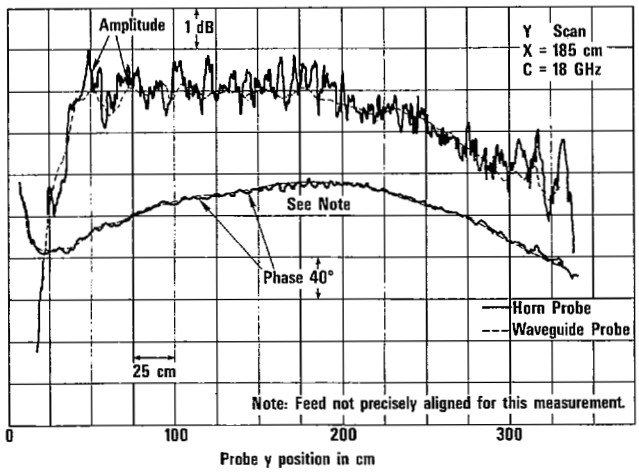

Fig. 17. Compact range main component, amplitude and phase, f = 18 GHz, horn and waveguide probe results under identical conditions.

horn probe, Figs. 9 and 10. This perhaps is more clearly demonstrated in Fig. 17 where horn and waveguide probe results are compared for a centerline y scan. (It should be noted that the results in Fig. 17 were obtained prior to the precise alignment of the feed at 18 GHz, but in fact show the quality of the variations.) It becomes apparent that these variations are the result of interfering fields caused by edge diffraction and feed spillover and that these fields are more severely attenuated by the narrower beam horn probe than by the broader beam waveguide probe. Various attempts to control these sources of variations did not produce significant changes in the results. Using the model discussed in Section IV, one might conclude from Fig. 17 that the direction of the interfering waves *in the test zone* is approximately 12°, which could imply that the probable sources are reflections from the base of the reflector. This overall problem should be investigated more fully to achieve optimum results.

D. Cross-Component Levels at 18.0 and 54.75 GHz

Cross-component levels can pose real problems for compact ranges since they affect both radar cross-section measurements and the direct measurement of antenna far-field patterns. To evaluate these levels, complete two-dimensional cross-component data were taken at 18.0 and 54.75 GHz. At 18.0 GHz, the cross-component levels in the 120 cm measurement plane of the test zone were typically in the order of 28 dB below the main component and are shown in the amplitude contour plots in Fig. 18. Phase contour plots were also made. The measured co- and cross-polarized data were also run through a computer program which computed polarization ratios and tilt angles to determine if the field of the compact range was actually more linearly polarized than 28 dB. Polarized ratios smaller than 28 dB would have indicated that the feed was rotated about its own axis so that the principal field component of the compact range was not parallel to the y-coordinate. The computed polarization ratios were typically in the order of 28 dB. Hence the feed was properly oriented.

At 54.75 GHz, cross-component amplitude and phase contours were also generated. Cross-component levels were typically 30–45 dB below the main component. Due to their rapid variation, contour plots for this case are difficult to distinguish and hence are not presented here.

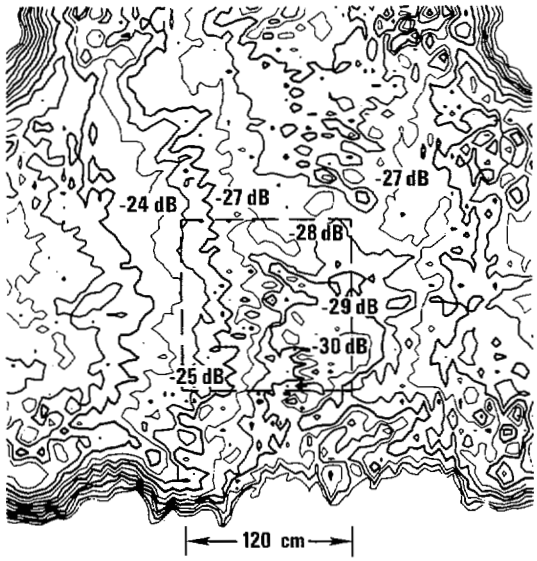

Fig. 18. Compact range cross component, 1 dB amplitude contours, one panel-support screw adjusted, f = 18 GHz, horn probe.

The cross-polarization levels in this (or any) compact range are affected by the feed-reflector geometry and by the polarization characteristics of the feed horns. However, even if one assumes that the feed horns are perfectly linear (they were not measured), and that the edges of the reflector and/or spaces between the reflector panels produce negligible depolarization, there is still a predicted nonzero cross component of about −30 dB due to this offset reflector's F/D ratio, see [5, Sec. II and Fig. 3]. This cross-polarization level is independent of frequency and hence would be expected at both 18 and 54.75 GHz, as the measured results indicate. These results should be investigated further.

CONCLUSION

The results of planar near-field measurements on this compact range demonstrate that an approximate plane wave illumination over a measurement zone 120 cm^2 with less

less than 0.5 dB amplitude variation and less than 10° phase variation can be achieved at frequencies approaching 60 GHz. The usefulness of this particular reflector design with precision panels and adjustable supports also has been demonstrated. In particular, the panel-support screw adjustment feature was effectively used to acquire phase variations 10° or less in the test zone at 54.75 GHz. In addition, this measurement program shows that planar near-field measurements are indeed practical and valuable in aligning and evaluating compact ranges because they provide more information than a limited number of analogue plots in one dimension. Contour plots of amplitude and phase data obtained from more complete two-dimensional measurements precisely and accurately locate sources of problems in the range reflector, with phase contour plots being more useful as diagnostic tools. The planar technique also provides a convenient way to measure cross-polarization levels precisely and accurately.

However, future work, both analytical and experimental, needs to be done to evaluate mm-wave ranges for radar cross section and antenna measurements. In particular the variations in the field caused by edge diffraction and feed spillover should be investigated under conditions approaching an ideal anechoic chamber so that each source of these residual variations may precisely be identified. In addition, before using the compact range as an *mm-calibration standard*, the effects of both the residual variations in the field and the cross-polarization levels on both radar cross-section measurements and the direct measurement of antenna far-field patterns should be accurately determined. A recommendation for future work in this area would involve calculating the spectrum of out-going waves for the compact range and trying to determine what errors in radar cross section and antenna pattern measurements could occur from the nonplane wave illumination of targets and antennas. If the errors are substantial, corrections to these measurements might be determined, resulting in more accurate measurements.

ACKNOWLEDGMENT

The authors wish to thank Allen C. Newell and Doren W. Hess for useful discussions and Robert B. Leighton for his help in obtaining and assembling the reflector.

REFERENCES

[1] D. W. Hess, F. G. Willwerth, and R. C. Johnson, "Compact range improvements and performance at 30 GHz," in *Digest Int. Symp.*, IEEE Antennas Propagat. Soc., June 20–22, 1977, Stanford Univ.

[2] A. C. Newell and A. G. Repjar, "Results of spherical near-field measurements on narrow-beam antennas," in *Digest Int. Symp.*, IEEE Antennas Propagat. Soc., June 20–22, 1977, Stanford Univ.

[3] A. C. Newell and M. L. Crawford, "Planar near-field measurements on high performance array antennas," Nat. Bur. Stand. (U.S.) Int. Rep. 380. July 1974.

[4] R. C. Johnson, H. A. Ecker, and J. S. Hollis, "Determination of far-field antenna patterns from near-field measurements," *Proc. IEEE*, vol. 61, no. 12, Dec. 1973.

[5] Ta-shing Chu and R. H. Turrin, "Properties of offset reflector antennas," in *Reflector Antennas*, A. W. Love, Ed. *IEEE Press*, 1978, pp. 212–218.

[6] R. B. Leighton, "A 10-meter telescope for millimeter and submillimeter astronomy," California Inst. Technol., Tech. Rep. for NSF, May 1978.

[7] J. S. Hollis, T. J. Lyon, and L. Clayton, Jr. *Microwave Antenna Measurements*. Atlanta, GA: Scientific-Atlanta, July 1970.

Andrew G. Repjar (M'77) was born in Timmins, ON, Canada, on November 14, 1941. He received the B.E.E., M.S., and Ph.D. degrees in electrical engineering from The Ohio State University, Columbus, OH, in 1964, 1966, and 1970, respectively.

In 1964 he became a Research Assistant in the Communications and Controls Systems Laboratory, Ohio State University, where his interests were in automated vehicular systems and pattern recognition. In 1967 he became a Research Associate in the ElectroScience Laboratory (formerly the Antenna Laboratory) at The Ohio State University where his interests were in the detection and identification of targets using radar techniques. In 1970 he became a Member of the Technical Staff at Rockwell International, Columbus, OH, where his primary interests were in the fields of antennas and microwaves. In 1975 he joined the Electromagnetics Division of the National Bureau of Standards, Boulder, CO, where he is currently utilizing near-field techniques for the determination of antenna parameters.

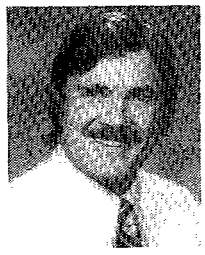

Douglas P. Kremer was born in Jefferson City, MO, on March 16, 1949. He is currently working toward the B.S.E.E. degree.

He has trained and has worked as an Electronics Technician in the U.S. Army. He joined the Antenna Systems Metrology Group in the National Bureau of Standards (NBS) Electromagnetic Fields Division in 1973 where he has been working for the past six years. Since joining NBS he has helped build the near-field scanner and associated equipment. He has been actively involved in all of the calibrations performed on it.